

Analysis of Dominant Process Parameters in Deep-Drawing of Paperboard

Tobias Müller,* Alexander Lenske, Marek Hauptmann, and Jens-Peter Majschak

The application of the wrinkle measuring method described in Müller *et al.* (2017) and the subsequent evaluation algorithm of a range of deep-drawn samples were used to determine the influences and interdependencies of blankholder force, tool temperatures, and drawing height on the formation of wrinkles in paperboard. The main influences were identified and quantitatively evaluated. For the given experimental space, a regression function was derived and validated in further experiments. It was shown that a quadratic regression was superior to the previously used linear regression. The findings were discussed and compared with the results of similar experiments from past publications. Special attention was given to the wrinkles formed and the resulting quality of the formed paperboard cups. The restrictions of the data acquisition from the measuring method that was used and limitations of the model were presented to demonstrate the reliability of the results.

Keywords: Paperboard; Deep-drawing; Forming; Process analysis; Quality assessment; Wrinkle distribution

Contact information: Chair of Processing Machines and Processing Technology, Technische Universität Dresden, Bergstrasse 120, 01069 Dresden Germany;

**Corresponding author:* tobias.mueller1@tu-dresden.de

INTRODUCTION

The quality of paperboard packaging components produced by deep-drawing is primarily measured by the number of wrinkles formed and uniformity of their distribution on the deep-drawn sample (Hauptmann 2010).

In the forming process, a blank is slid between the forming matrix and a blankholder. The blankholder then clamps the material on the matrix with a defined but changeable force. In the next step, the drawing punch drives into the matrix and draws the material along. The deep-drawn part can then be ejected from the matrix. During the forming process, the wrinkle distribution can be influenced by the tool temperature, blankholder force, blankholder force profile, and compression in the forming gap (Hauptmann 2010). There are further influences, such as different materials or climate conditions, but these are not reviewed in this work.

The wrinkle distribution of the deep-drawn paperboard sample was measured by laser topography. For this purpose, the sample was mounted on a rotary plate and scanned by a triangulation laser. The profile of the laser measurement was then evaluated for wrinkles, as described in the work of Müller *et al.* (2017).

For a better understanding of the mechanisms involved in the forming of wrinkles during deep-drawing, it is important to understand the primary influencing parameters. This work aims to experimentally identify those parameters and model the general wrinkle-forming behavior accordingly. For this purpose an experimental study that links

the influencing parameters to the resulting wrinkle distributions is performed as described below.

EXPERIMENTAL

Method and Setup

The experiments were performed at the deepdrawing testrig at Dresden University of Technology. For each experiment the testrig was set up with the specific parameters (Table 2) for the measurement point. Next the paperboard blank was inserted between the blankholder and the forming matrix as shown in Fig. 1. The blank was then clamped by the blankholder with a predefined force-profile as given in Fig. 2. The punch then pulled the material into the forming matrix in the downstroke. After forming the paperboard cup and pulling the sample all the way through the matrix, the punch moved back up again and shed the formed sample at the bottom edge of the matrix. The sample was then extracted and examined for its wrinkle distribution.

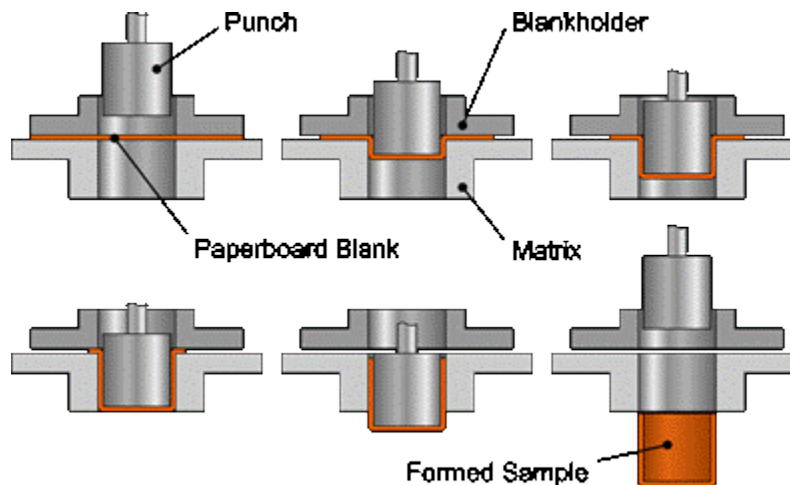


Fig. 1. Deepdrawing of paperboard process (top left to bottom right): Insert and clamping of the blank, forming with wrinkle compression between punch and matrix, formed sample.

The method described in Müller *et al.* (2017) was used to obtain the wrinkle distributions for a multitude of samples. The process parameters of the sample productions had various applied blankholder forces, matrix temperatures, and forming punch temperatures. Other influential parameters were held at a constant level, as can be seen in Table 1.

Table 1. Constant Parameters during the Experiment

Climate	Forming Speed & Height	Material	Forming Clearance (Gap Width)	Geometry
25 °C; 50% Rel. Humidity	$v_f = 20$ mm/s $h_f = 25$ mm	Stora Enso Trayforma Natura 350 g/m ²	0.35 mm	Round, diameter Ø110 mm

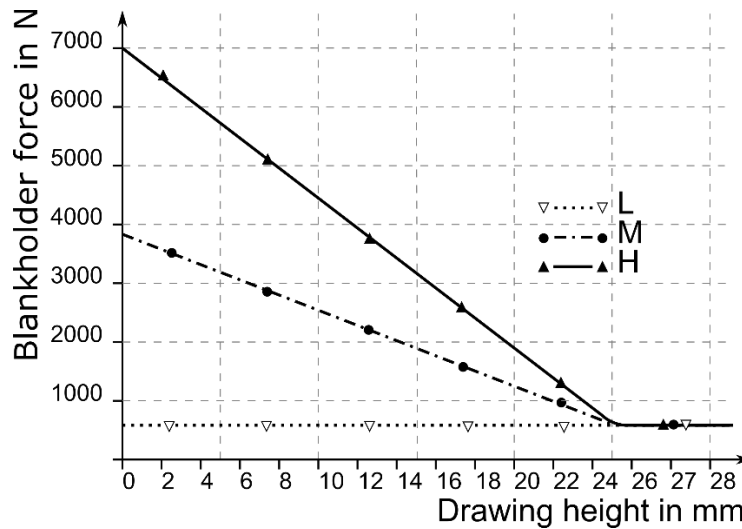


Fig. 2. Profiles of the blankholder force with respect to the forming height at low (L), medium (M), and high (H) levels

The blankholder force (F_{bh}) was applied fully at the beginning of the drawing process and reduced to a F_1 of 500 N at a drawing height (h_1) of 25 mm, which can be seen in Fig. 2. The variable F_{bh} was calculated from Eq. 1,

$$F_{bh}(x) = F_0 - \frac{F_0 - F_1}{h_1} \cdot h(x) \quad (1)$$

where $h(x)$ is the current drawing height (mm), h_1 is the maximum drawing height (mm), and F_1 is the blankholder force (N) at the maximum drawing height. The variable F_0 is the initial blankholder force (N), and its values are given in Table 2.

This ensured that during the deep-drawing process, the remaining material between the blankholder and matrix was applied with an approximately constant pressure almost up to the final drawing height (Hauptmann *et al.* 2016). The blankholder force (F_{bh}) shall be denoted by the initial, maximal blankholder force (F_0) hereafter.

The temperatures of the matrix (T_{mx}) and the forming punch (T_{pn}) were constant during each drawing process and only varied between measurements.

The three influencing parameters, F_{bh} ($= F_0$), T_{mx} , and T_{pn} , were varied according to a fully factored Design of Experiment with median levels (Siebertz *et al.* 2010), as summarized in Table 2.

Table 2. Variation Levels of the Influencing Parameters

Level (Simplified)	Blankholder Force (F_0)	Matrix Temperature (T_{mx})	Punch Temperature (T_{pn})
Low (L)	500 N	80 °C	80 °C
Medium (M)	3750 N	100 °C	100 °C
High (H)	7000 N	120 °C	120 °C

The resulting experiment was conducted at 27 different measurement points with eight individual measurements at each point to acquire statistical dependability, while limiting the experimental complexity to a reasonable level.

RESULTS AND DISCUSSION

Model and General Influences

The volume of the obtained experimental data permitted the postulation of a complex, linear-quadratic regression model, Eq. 2,

$$y = \alpha_0 + \alpha_1 \cdot T_{mx} + \alpha_2 \cdot T_{pn} + \alpha_3 \cdot F_{bh} + \alpha_4 \cdot T_{mx} \cdot T_{pn} + \alpha_5 \cdot T_{mx} \cdot F_{bh} + \alpha_6 \cdot T_{pn} \cdot F_{bh} + \alpha_7 \cdot T_{mx}^2 + \alpha_8 \cdot T_{pn}^2 + \alpha_9 \cdot F_{bh}^2 \quad (2)$$

where y denotes the target parameter (number of wrinkles, standard deviation of wrinkle distances). The variables T_{mx} , T_{pn} , and F_{bh} are the influencing parameters matrix temperature (°C), punch temperature (°C), and initial blankholder force (N), respectively. The coefficient α_i indicates the strength of the influencing parameters in the model and needed to be determined experimentally.

The experimental data for the middle points in the experimental space were used to determine if a linear model can be consistently verified. However, the linear model was not sufficient for all influences, and it was shown that the quadratic model was more consistent with the measured data.

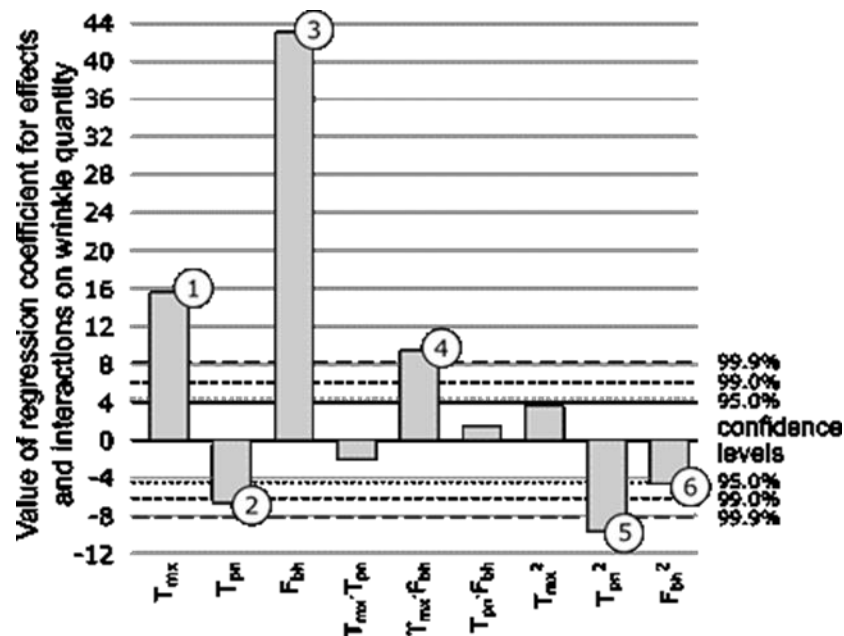


Fig. 3. Summary of the relevant influence parameters and the quantitative value of the influence on the wrinkle quantity at a h of 20 mm

An evaluation of the regression-coefficients yielded the significance of each effect or interaction of effects. The regression values ($= 2 \cdot \alpha_i$) for the dependent variable wrinkle quantity are displayed in Fig. 3. The following observations were obtained:

- (1) The temperature of the matrix had a highly significant (p -value < 0.001) and positive effect on the wrinkle quantity. The higher temperatures of the matrix yielded higher wrinkle quantities. This effect was confirmed by Wallmeier *et al.* (2015).
- (2) The temperature of the forming punch had a very significant (p -value < 0.01) and negative effect on the wrinkle quantity. This effect was not observed in previous

works and may have been masked by the thermal expansion of the tools and the resulting change in the forming gap. These implications are addressed below.

- (3) The blankholder force had a highly significant and positive effect on the wrinkle quantity. The effect of the blankholder force was the dominant effect on the wrinkle quantity. This was in accordance with Hauptmann (2010) and Wallmeier *et al.* (2015). The excess material during forming was pushed into more, but finer wrinkles at higher blankholder forces.
- (4) The interaction of T_{mx} and F_{bh} had a highly significant and positive effect on the wrinkle quantity. Therefore, it was confirmed that the beneficial effects of the increased blankholder force and matrix temperature were not mutually exclusive and were present simultaneously.
- (5) The quadratic temperature of the forming punch (T_{pn}^2) had a highly significant and negative influence on the wrinkle quantity. This showed that the effect of the punch temperature increased quadratically and did not level off. Again, these implications were discussed below.
- (6) The quadratic blankholder force (F_{bh}^2) had a significantly negative influence on the wrinkle quantity. This effect displayed the saturation effect of the wrinkle quantity at high wrinkle counts (*cf.* Fig. 6, Fig. 12, and Wallmeier *et al.* 2015, Fig. 7).

All other examined parameter combinations showed no significant effects on the wrinkle quantity.

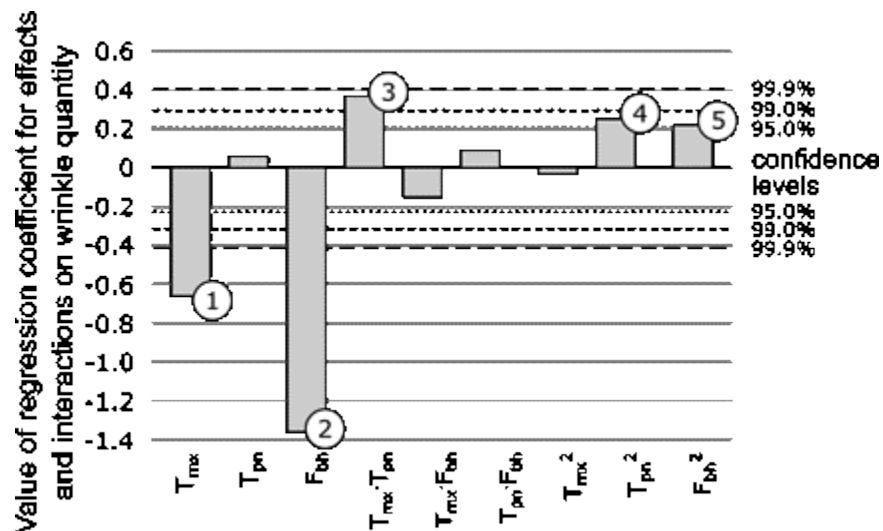


Fig. 4. Summary of the relevant influence parameters and the quantitative value of the influence on the standard deviation of the wrinkle distances per wrinkle at an h of 20 mm

For the measure of the evenness of the wrinkle distribution, the standard deviation of the distances between the wrinkles on the samples was adducted. Because the wrinkle distances and the corresponding deviations are linearly connected to the quantity of wrinkles at each measure point, the standard deviation of the wrinkle distances was divided by the total amount of wrinkles present at each measurement point. This ensured a general comparability between different samples, as well as different drawing heights. Conclusively, the evenness was defined as the reciprocal of the standard deviation of the

distances between individual wrinkles (σ_{dist}) per number of wrinkles (n) on the corresponding samples, as shown in Eq. 3,

$$evenness := \left(\frac{n}{\sigma_{dist}} \right) \quad (3)$$

The regression values for the dependent variable standard deviation of wrinkle distances per wrinkle (σ_{dist}/n) are displayed in Fig. 4. The following observations were made:

- (1) The temperature of the matrix had a highly significant ($p < 0.001$) and negative effect on the (σ_{dist}/n) (*i.e.* higher T_{mx} values yielded lower (σ_{dist}/n) values).
- (2) The blankholder force had a highly significant and negative effect on the (σ_{dist}/n). The effect of the blankholder force was the dominant effect on the (σ_{dist}/n). This confirmed the influence that had been established in Hauptmann (2010).
- (3) The interaction of T_{mx} and T_{pn} had a very significant and positive effect on the (σ_{dist}/n). While not directly comparable, a similar effect had been found by Hauptmann (2010) for the difference of the tool temperatures ($\Delta T = |T_{mx} - T_{pn}| = f(T_{mx}, T_{pn})$).
- (4) The quadratic temperature of the forming punch (T_{pn}^2) had a significant (p -value < 0.05) influence on the (σ_{dist}/n).
- (5) The quadratic blankholder force (F_{bh}^2) had a significant influence on the (σ_{dist}/n). This confirmed the previously mentioned wrinkle saturation effect (*cf.* Fig. 60 in Hauptmann 2010 and Fig. 7 in Wallmeier *et al.* 2015).

All other examined parameter combinations showed no significant effects on the (σ_{dist}/n).

For a simplified representation of the occurring effects, three parameter-levels, low (L), medium (M), and high (H), were selected, as shown in Table 2.

The samples were examined for the disparity of the material elongation according to the material anisotropy and for the distinct change of wrinkle distribution with increased drawing height. Furthermore, the effects of the blankholder force and temperature of the matrix were studied in detail. The process-physical implications are discussed along with the experimental findings.

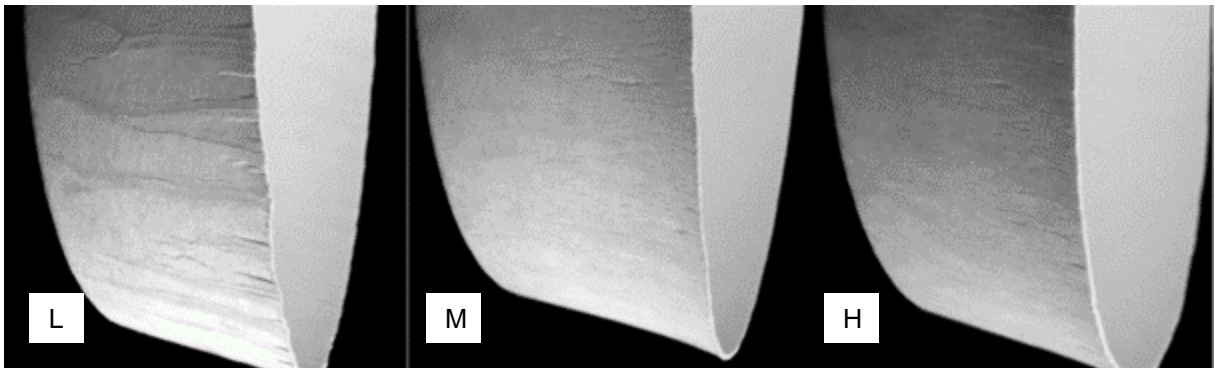


Fig. 5. Comparison of the samples at the simplified levels L ($T_{mx} = 80$ °C, $T_{pn} = 80$ °C, $F_0 = 500$ N), M ($T_{mx} = 100$ °C, $T_{pn} = 100$ °C, $F_0 = 3750$ N), and H ($T_{mx} = 120$ °C, $T_{pn} = 120$ °C, $F_0 = 7000$ N)

The general variation of the quality-level in the samples can be seen in Fig. 5. On the other hand, Fig. 5 (left) displayed very rough and easily detectable wrinkle structures, and the structures in Fig. 5 (middle) and Fig. 5 (right) were increasingly finer, more even, and therefore, harder to detect.

Effect of the Material Anisotropy

Because paperboard exhibits a strong anisotropy and differing material properties in the machine direction (MD) and cross direction (CD), the quality of the samples also varied in the MD and CD. This was especially apparent during the examination of the form distinctness of the wall section of the samples.

Figure 6 displays the general difference of the elongation-behavior in the MD and CD for increasing drawing heights. The elongation in the CD was significantly higher than in the MD. The elastoplastic displacement was exhausted early in the process. It was identified that the relative elongation decreased with increasing drawing height for MD and CD alike until a saturation is reached when no more elastoplastic behavior takes place. This behavior confirms the limited elastoplastic properties of paperboard (Vishtal and Retulainen 2012).

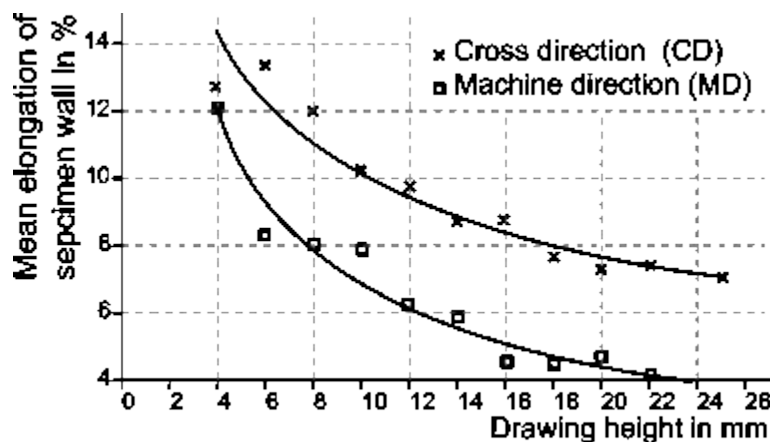


Fig. 6. Relative mean wall elongation as an effect of the drawing height ($n = 16$ for each set). It was measured individually for each drawing height with $T_{mx} = 120$ °C, $T_{pn} = 120$ °C, and $F_{bh} = 7000$ N.

Effect of the Drawing Height

The absolute wrinkle quantity increased with increasing drawing height (Fig. 7). However, the total wrinkle quantity leveled off at a drawing height of approximately 24 mm, or 330 wrinkles.

The asymptotic quantity of wrinkles was observed along all parameter levels. The maximum amount of wrinkles was reached when the mean distance between individual wrinkles reached 1000 to 1200 μm . After reaching the maximum amount of wrinkles, the excess material during the deep-drawing process was added to already existing wrinkles and almost no new wrinkles were formed (*cf.* Wallmeier *et al.* 2015).

Whilst Fig. 6 revealed the correlation between material orientation and the mean material elongation during the deep-drawing process, Fig. 8 exposes the different behavior of the material at the different parameter levels on the mean elongation of the walls of the samples. The main influence was attributed to the applied blankholder force. It was confirmed, the relative mean elongation decreased with the drawing height and the

elongation increased with the applied blankholder force. However, both effects were superimposed with many outliers, especially at lower drawing heights. Furthermore, the true magnitude of the individual effect was partially masked by the simultaneous variation of the three parameters T_{mx} , T_{pn} , and F_{bh} .

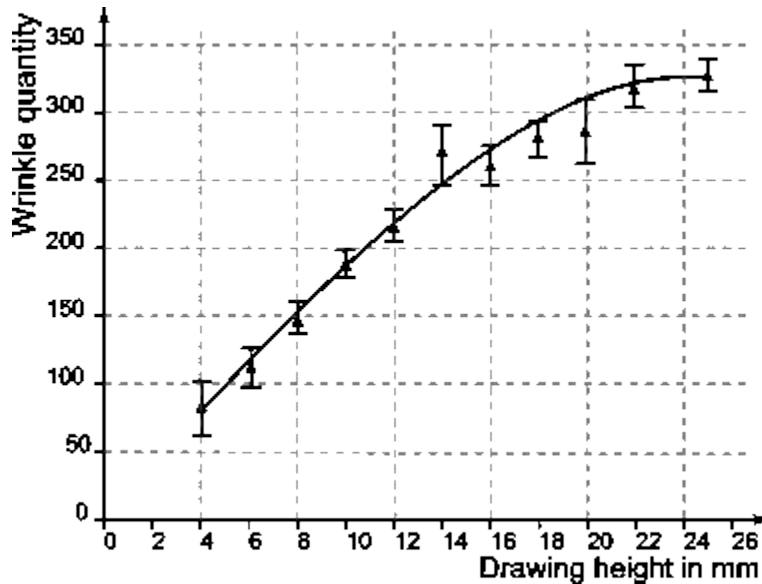


Fig. 7. Wrinkle quantity as an effect of the drawing height ($n = 24$ for each set). It was measured individually for each drawing height with $T_{mx} = 120$ °C, $T_{pn} = 120$ °C, and $F_{bh} = 7000$ N.

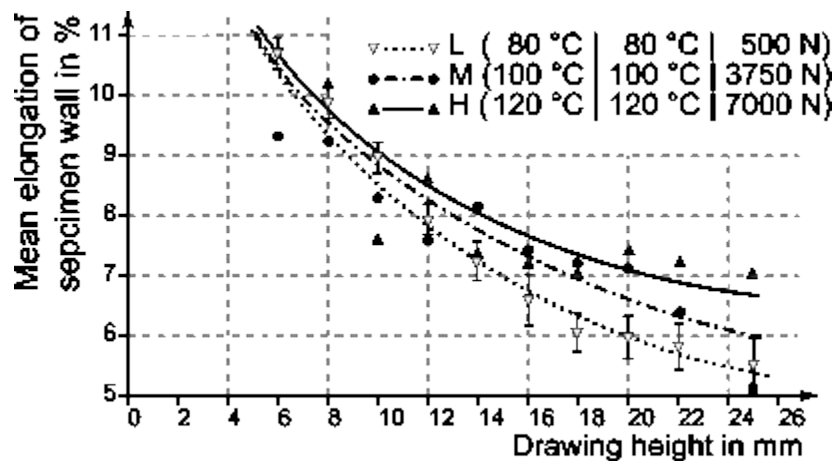


Fig. 8. Relative mean wall elongation as an effect of the drawing height at different parameter levels ($n = 8$ for each)

The cutoff of the graph below the 4 mm drawing height was caused by the restrictions of the measuring method. The samples exhibited strong curvatures at the bottom, which impeded true measurements. Furthermore, the wrinkles were just beginning to form between 2 mm to 4 mm (Müller *et al.* 2017). Therefore, in this experiment, the wrinkle structures at the low drawing heights did not exist or were very delicate and often below the detection threshold of the measuring method. Thus, the error-prone data below 4 mm was cropped from the evaluated data. Further studies should include an examination of the initial wrinkle forming.

Effect of the Applied Blankholder Force

The combined influences of the blankholder force and the temperature of the matrix on the wrinkle quantity and the evenness of the wrinkle distribution are displayed in Fig. 9. The temperature of the forming punch was kept at a constant level of 90 °C. It was later shown that this level was close to the optimum within the evaluated parameter space.

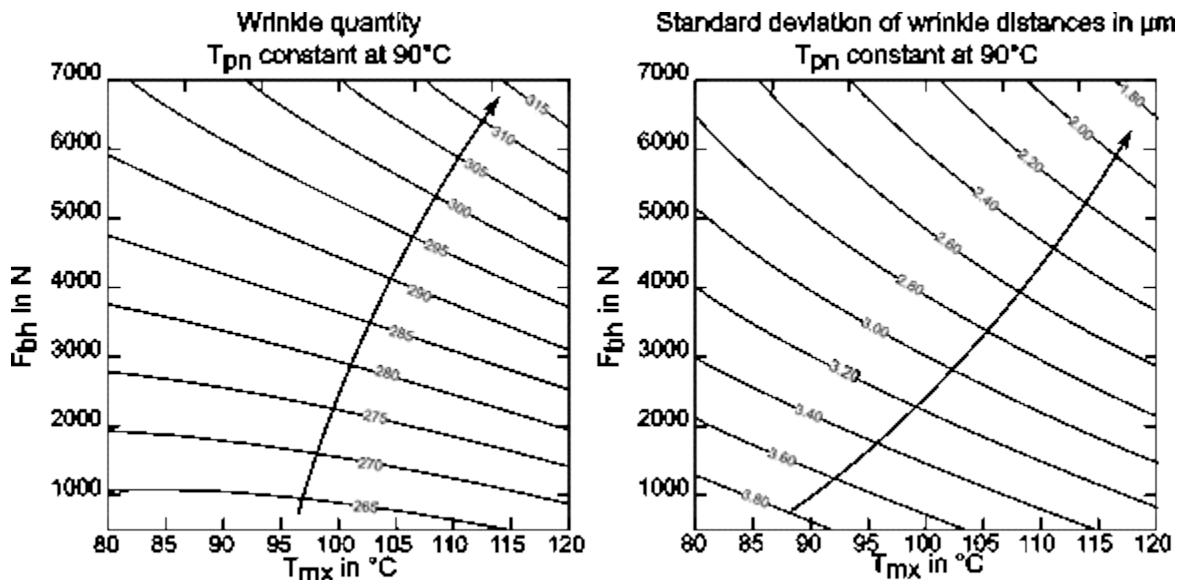


Fig. 9. Wrinkle quantity as an effect of the blankholder force and matrix temperature ($n = 8$ for each data point). The optima for both graphs are in the upper right corner.

The examination of the contour diagrams showed that a high blankholder force in combination with high temperatures of the matrix yielded the best results for wrinkle quantities, as well as for the wrinkle distribution. Furthermore, it was observed that the influence of the blankholder force was vastly dominant over the temperature influence at low force levels. The impact of the temperature of the matrix increased with higher blankholder forces. The gradient shifted towards the temperature axis in the upper right corner, which signified a larger influence by the temperature.

Effect of the Tool Temperature

The combined influences of the temperature of the matrix and forming punch on the wrinkle quantity and the evenness of the wrinkle distribution are displayed in Fig. 10. The blankholder force was kept at a constant level of 7000 N, and as shown in Fig. 9, this was the optimum within the explored parameter space.

The contour plots in Fig. 10 revealed that the influence of the T_{mx} was significantly higher than the influence of the T_{pn} . Furthermore, the curved lines indicated that the influence of the T_{pn} included a quadratic term. Interestingly, the optimal parameters for a high wrinkle quantity were not found at one of the corners of the diagram, but rather on the right side at a T_{mx} of approximately 120 °C and a T_{pn} of approximately 90 °C.

The deviation of the wrinkle distances per wrinkle exhibited the parameter optimum at a T_{mx} of approximately 120 °C and a T_{pn} of approximately 80 °C. However,

the non-linear behavior of the wrinkle-response and the deviation-response to the influence parameters leave room for interpretation.

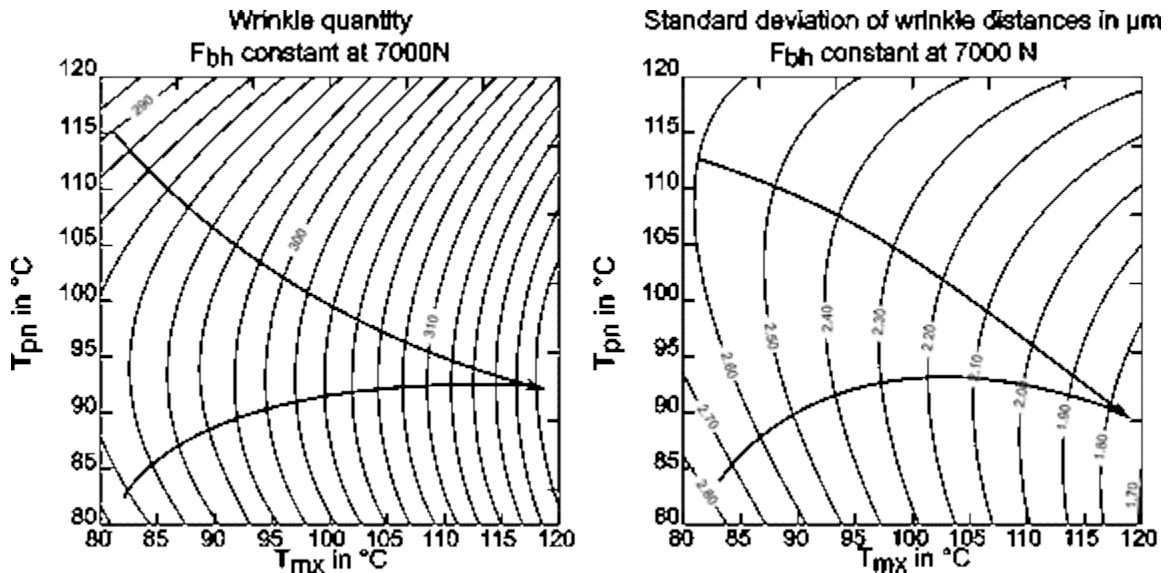


Fig. 10. Wrinkle quantity and wrinkle distribution as an effect of the blankholder force and matrix temperature

The evaluation of the main influence parameters revealed that the punch temperature only faintly affected the wrinkle distribution. However, the temperature of the forming matrix had a major impact on the wrinkle distribution. As viewed in Fig. 9, the evenness of the wrinkle distribution measured by the standard deviation of the wrinkle spacing did not yield the expected results. It was deduced that the wrinkle distribution became smoother as more wrinkles formed at higher forming heights. The high level exhibited a higher deviation at low forming heights since the forming of wrinkles was delayed at higher parameter levels (*cf.* Hauptmann *et al.* 2016, Fig.12b).

However, it was taken into consideration that the temperatures of the matrix and forming punch directly influenced the effective width of the forming gap (s_{gap}). This was according to Eq. 4,

$$s_{gap} = \frac{1}{2} \cdot \left(l_{0,mx} \cdot (1 + \alpha \cdot \Delta T_{mx}) - l_{0,pn} \cdot (1 + \alpha \cdot \Delta T_{pn}) \right) \quad (4)$$

where $l_{0,mx}$ (110 mm) and $l_{0,pn}$ (109.3 mm) are the diameters (mm) of the matrix and forming punch at room temperature, 297 K (= 25 °C), respectively. The variables ΔT_{mx} and ΔT_{pn} are the temperature differences of the matrix and forming punch in regards to the reference room temperature, respectively. An α of $13.0e^{-6} \text{ K}^{-1}$ is the coefficient of thermal expansion for the tool material (steel) (Cverna 2002).

Within the examined parameter space (Table 1), a range of widths in the forming gap, from 0.32 to 0.38 mm, was possible. A high material (and wrinkle) compression was achieved at high levels of punch temperature and low levels of matrix temperature (see Fig. 10, upper left corner). After an assessment of the measuring method was taken into consideration, it was deduced that some wrinkles may not have been detected at high levels of compression. Therefore, the strong quadratic behavior originating in the top left corner of Fig. 10 might have been caused by the decreased amount of wrinkles detected,

even though more wrinkles were actually present. A sensible explanation for the quadratic term was that at low to medium compressions, the behavior was quasi-linear, and at high compressions, the behavior became more and more quadratic because fewer wrinkles were detected by the proposed method.

Considering the results displayed in Fig. 10 and the discussion above, it was insightful to examine the wrinkle quantity at each measuring point and scale the unevenness of the wrinkle spacing to the wrinkle quantity accordingly. Furthermore, it was demonstrative to juxtapose the wrinkle data in the MD and CD to display the total amount of wrinkles and reveal the anisotropy-induced differences in both directions (see Fig. 11).

Nevertheless, the interpretation of an effect of the width of the forming gap on the actual present wrinkle distribution was not permissible. The width of the forming gap could not have an influence on the actual wrinkle distribution because by the time that the material was drawn into the forming gap, all of the wrinkles had already been formed between the matrix plate and the blankholder plate. The width of the forming gap only influenced the extent of compression the wrinkle structures experienced during the forming process. Especially with high wrinkle quantities and very fine wrinkle structures, this effect led to even finer wrinkles, which could not be detected by the algorithm. An apparent, but not actual, decrease of the wrinkle quantity with a smaller forming gap was observed (Figs. 11 and 12).

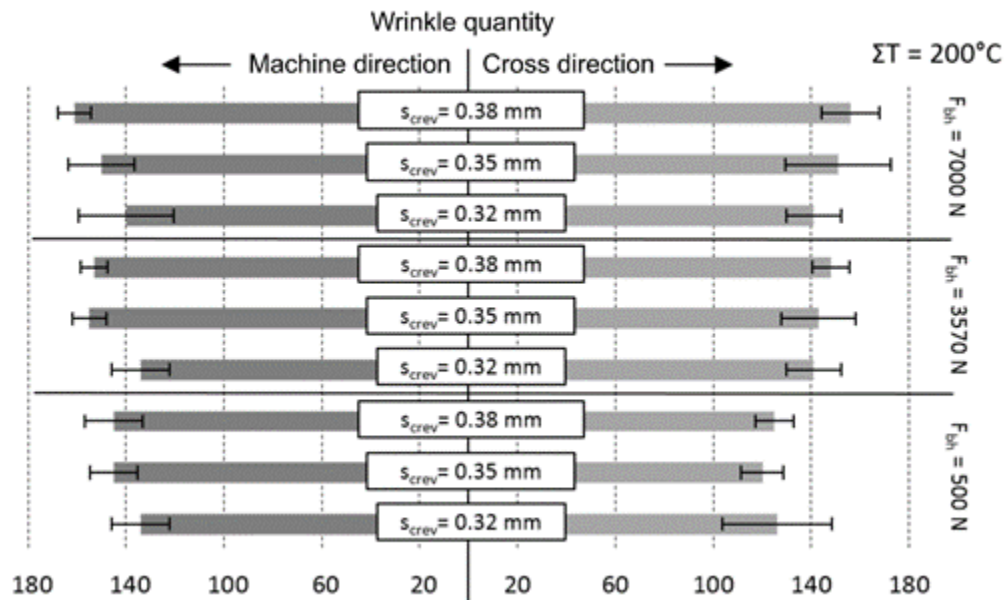


Fig. 11. Wrinkle quantity for the different blankholder forces and effective forming gaps ($n = 8$ for each subset)

Figure 11 depicts the total wrinkle quantity in the MD and CD at a constant temperature sum ($\Sigma T = T_{mx} + T_{pn}$) for the different widths of the forming gap and different blankholder forces. The temperature sum was kept at a constant level of 200 °C to avoid influences by different energy absorption of the paperboard material. It was apparent that the total wrinkle quantity rose with higher blankholder forces. While the distribution of the wrinkles was slightly tilted towards the MD at lower blankholder forces, the distribution seemed to equalize at higher levels. Furthermore, it was deduced

that a greater width of the forming gap allowed for more wrinkles to form, though this did not hold true for all of the measurement points. The chance cannot be dismissed that some wrinkles eluded detection after high compression in a tight forming gap, as has been previously discussed.

The evenness of the wrinkle distribution, as measured by the standard deviation for the wrinkle distances per wrinkle, is displayed in Fig. 12. It was obvious that the wrinkle distribution, especially at low blankholder forces, was much more uneven in the CD than in the MD. Concerning the influence of the width of the forming gap on the evenness of the wrinkle distribution, a slight disposition towards a higher level of evenness at wide gaps was suspected. The tight forming gap (*i.e.*, $s_{gap} = 0.32$ mm) resulted in an increased compression of existing wrinkles so that fewer wrinkles were detectable by the proposed method. It was measured that the average surface roughness (R_z) of the used paperboard decreased from approximately 14 μm before the forming process to approximately 6 μm after the forming process. This effect was beneficial for the wrinkle detection at low compression levels since the separation of individual wrinkles and surface roughness was facilitated. However, at high compression levels, even the wrinkles were compressed and smoothed so intensely that reliable wrinkle-detection was hindered.

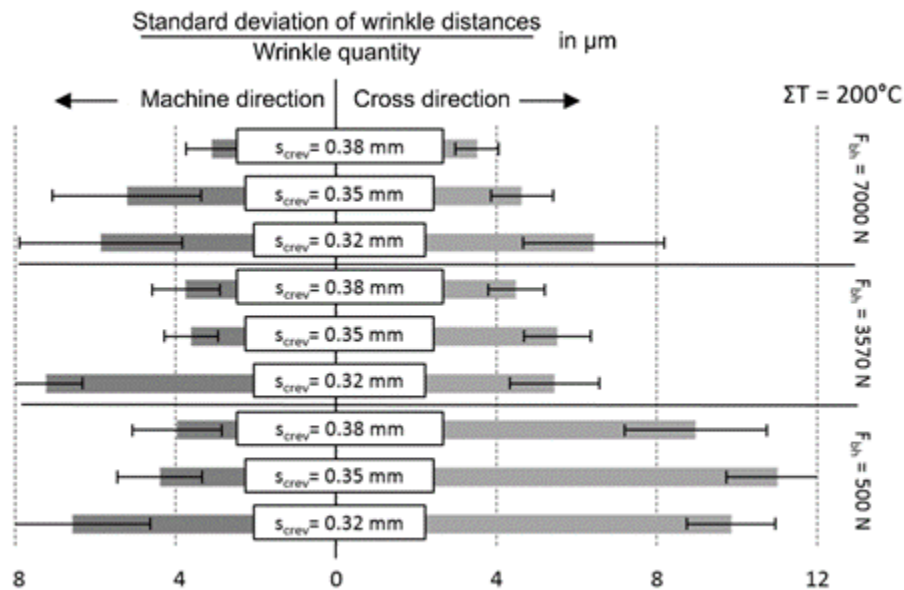


Fig. 12. Standard deviation of the mean wrinkle distances relative to the wrinkle quantity for the different blankholder forces and effective forming gaps ($n = 8$ for each subset)

No significant influence of the temperature sum was measured within the range of 180 to 220 $^\circ\text{C}$. However, the examined range embodied only a fraction of the possible temperature spectrum, and so further studies are advisable.

Effect on the Sample Quality

The overall sample quality is a combination of optical quality, stability, geometric retention, and absence of local material failures (Hauptmann 2010). Hauptmann and Majschak (2011) suggest contracting individual quality parameters into an overall quality measure (Q). This approach includes a broad range of quality decreasing features and can

obtain paramount accuracy. However, the necessary measurements are very time consuming and prohibit an application of the method for studies with extensive amounts of measurement points.

The method described in this paper only obtained the wrinkle quantity (n) and the separation distances between individual wrinkles (d_{ij} , mm unit). The wrinkle quantity can be utilized directly. The separation distances can be used to calculate the mean separation distance (\hat{d} , mm unit) and the evenness of the wrinkle distribution with Eq. 5,

$$\text{evenness} = \frac{n}{\sigma_{dist}} = \frac{n^2}{\sqrt{n \cdot \sum_{l=1, j=2}^{n-1, n} d_{lj}} - \hat{d}} \quad (5)$$

To effectively utilize the determined quality values in an experimental setting with a high number of measurement points or for industrial quality assurance, the wrinkle quantity and evenness had to be condensed into a single quality value (Q), similar to Hauptmann and Majschak (2011). The single values were weighted to account for their attribution towards a high quality. Because the wrinkle quantity was the primary target figure¹, it was weighted higher than the evenness. To determine the arbitrary weights, the significance levels of the main influencing value, the blankholder force, was used. While the influence of the blankholder force on the wrinkle quantity was about five times higher than the 99.9% level, it was only about three times higher than the 99.9% level for the evenness (Figs. 11 and 12). A weight ratio of 5:3 seemed sensible. This ratio had to be scaled to the absolute values of the two measurement values n and (σ_{dist}/n) . The scaling factors were taken from the asymptotic values of a n_{norm} of 330 wrinkles and $(\sigma_{dist}/n)_{norm} = 1.5 \mu\text{m}$ per wrinkle. Finally, the sign of the influence had to be taken into account. To achieve a high quality level, many wrinkles are needed, and therefore, the sign of the wrinkle-quality-term had to be positive (+). For a high quality, an even wrinkle distribution is required, and therefore, a high value of evenness was required. However, the evenness is the reciprocal of (σ_{dist}/n) , and therefore, the sign had to change to negative (-) when using (σ_{dist}/n) for the calculation of the overall quality. With the aforementioned considerations, the overall quality value was expressed by Eq. 6,

$$Q = +\frac{1}{66} \cdot n - 2 \cdot \frac{\sigma_{dist}}{n} ; (-10 \leq Q \leq 2) \quad (6)$$

The range of the possible quality-values Q was picked, so that the arbitrary threshold for a sufficient quality level is at 0. Positive values for Q mark samples with a desirable quality, while negative values denote samples of insufficient quality.

Limitations and Future Studies

In Fig. 13 it was observed that a high initial blankholder force of 7000 N seemed to inhibit the forming of wrinkles in favor of increased elastoplastic behavior (see Fig. 6). At higher drawing heights, a high blankholder force generated an increased amount of wrinkles compared to the lower levels of the blankholder force. The behavior of a medium level blankholder force at low drawing heights was curious since the highest amount of wrinkles were detected, which was much higher than the amount of wrinkles formed at the low level blankholder force. It had been expected that the wrinkle quantity

¹ This is true for most experimental studies. Some studies may emphasize the evenness and the differences in the MD and CD. The weights should then be adjusted accordingly.

of the H-level should be considerably higher than that of the M-level at moderate drawing heights of approximately 10 mm (Fig. 13). As already discussed, the reason for this observation might have been that a non-negligible amount of wrinkles was not detectable at the H-level. This led to the assumption that a minimum wrinkle dimension is necessary for a reliable detection. Examination of the applied method and the validation of the results with alternative measurement methods showed that the minimum wrinkle dimension for successful and reproducible detection was at a wrinkle width of approximately 8 μm to 12 μm .

For the measurement of the wrinkle distribution, the samples had to be attached to a manipulator. For round symmetrical samples, the manipulator just rotated the samples, so that the scanning laser could obtain the topography at the appointed height-level. For other geometries, a more complex manipulation was necessary. The limitations concerned with the measuring device are described in detail in Müller *et al.* (2017).

Taking into account the fixation of the samples into the measuring device and the rising complexity levels for non-round samples, a fast and reliable measurement may not be feasible in all cases.

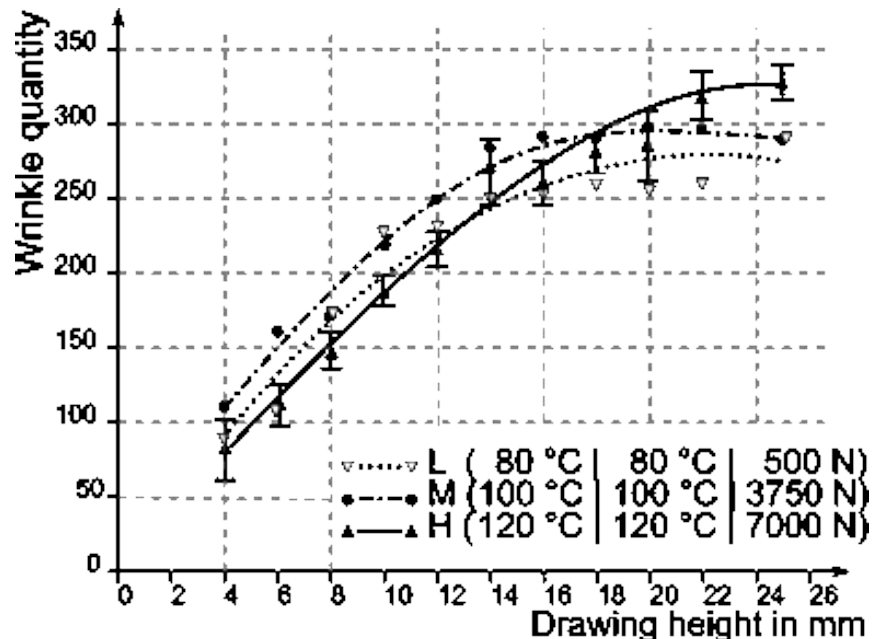


Fig. 13. Wrinkle quantity as an effect of the drawing height ($n = 8$ for each subset). It was measured individually for each drawing height. The figure illustrates the limitation of the detection resolution for very small wrinkle dimensions at high parameter levels.

Furthermore, the scanning laser only obtained the topography of one height-level at a time. The measurement takes many iterations and the advantage of the measuring speed for a single height-level cannot be upheld for the entire samples height, especially for studies including an analysis of the progress of the wrinkles from the bottom to the top of the wall section of the samples.

CONCLUSIONS

The analysis of the wrinkle data for different drawing heights provided valuable insights into the mechanics of wrinkle generation. It was shown that the material initially formed very few wrinkles and there was more elastoplastic deformation. With an increasing drawing height, more wrinkles were formed. However, there seemed to be a peak value for the wrinkle quantity at approximately 330 wrinkles for the examined samples. This was explained by a saturation effect in the walls of the samples. At a sufficient saturation of the samples with wrinkles, new wrinkles were not formed between existing wrinkles, but rather the additional material was added to the existing wrinkles.

Connecting the wrinkle data with the applied process parameters showed the intensity of each influencing parameter. It was confirmed that the main influence was the blankholder force (Wallmeier *et al.* 2015). An additional influence was attributed to the temperature of the matrix. However, a significant influence of the temperature of the forming punch could not be confirmed.

The key findings of this work are as follows:

1. Within the experimental space, wrinkle development increased linearly with drawing height until a saturation level at a forming ratio of approximately 0.15 was reached. Any surplus material was added to already existing wrinkles.
2. An increased blankholder force led to the development of an increased number of wrinkles. High forces induced a fine and evenly distributed wrinkle arrangement. However, the blank holder force was limited by the tensile strength of the paperboard material.
3. A high temperature of the forming matrix further improved the wrinkle distribution towards fine and evenly distributed wrinkle arrangements.
4. Contrary to previous studies, an effect of different punch temperatures on the wrinkle distribution could not be verified outside the influence of the temperature on the width of the forming gap.
5. While the wrinkle quantity in the machine direction and cross direction did not vary much, wrinkles in the cross direction were significantly more uneven.
6. The given observations can be used to obtain an improved quality level of deep-drawn paperboard containers. Applying the highest tolerable blankholder force and the highest sufferable temperature of the forming matrix leads to an improved quality of the samples. The blankholder force and temperature are limited by the paperboard failure behavior. A fine tuning of the wrinkle distribution can be achieved by utilizing the effect of the punch temperature on the forming gap, and therefore, the compression of the material during deep-drawing.
7. Examining the influence of the temperature sum (*i.e.* thermic energy applied to the material) did not yield significant results. However, the examined temperature range was too small to convey this indifference generally.
8. The limits of the proposed method included a deficiency at detecting very delicate wrinkle structures or highly compressed wrinkles. This led to errors in the evaluation of the influences of the parameters, especially the temperature of the forming punch.

This was because the punch had no direct influence on the formation of wrinkles, but could assist in masking wrinkles through high compression in the forming gap.

ACKNOWLEDGMENTS

The authors gratefully acknowledge the support of the Research Group “Forming of Fiber-Based Materials” at Technische Universität Dresden, and thank Stora Enso for supplying the material.

REFERENCES CITED

- Cverna, F. (2002). *ASM Ready Reference: Thermal Properties of Metals*, ASM International, Materials Park, OH.
- Hauptmann, M. (2010). *Die Gezielte Prozessführung und Möglichkeiten zur Prozessüberwachung beim Mehrdimensionalen Umformen von Karton durch Ziehen*, [Directed Process-Control for the 3D-Forming of Paperboard by Deepdrawing] Ph.D. Dissertation, Technical University Dresden, Dresden, Germany.
- Hauptmann, M., and Majschak, J.-P. (2011). “New quality level of packaging components from paperboard through technology improvement in 3D forming,” *Packag. Technol. Sci.* 24(7), 419-432. DOI: 10.1002/pts.941
- Hauptmann, M., Weyhe, J., and Majschak, J.-P. (2016). “Optimisation of deep drawn paperboard structures by adaptation of the blank holder force trajectory,” *J. Mater. Process. Tech.* 232, 142-152. DOI: 10.1016/j.jmatprotec.2016.02.007
- Müller, T., Lenske, A., Hauptmann, M., and Majschak, J.-P. (2017). “Method for fast quality evaluation of deep-drawn paperboard packaging components,” Submitted for publication in: *Packag. Technol. Sci.*
- Siebertz, K., van Bebber, D., and Hochkirchen, T. (2010). *Statistische Versuchsplanung: Design of Experiments (DoE)* [Statistical Experimental Planning: Design of Experiments], Springer-Verlag, Berlin, Germany.
- Vishtal, A., and Retulainen, E. (2012). “Deep-drawing of paper and paperboard: The role of material properties,” *BioResources* 7(3), 4424-4450. DOI: 10.15376/biores.7.3.4424-4450
- Wallmeier, M., Hauptmann, M., and Majschak, J.-P. (2015). “New methods for quality analysis of deep-drawn packaging components from paperboard,” *Packag. Technol. Sci.* 28(2), 91-100. DOI: 10.1002/pts.2091

Article submitted: January 26, 2017; Peer review completed: March 5, 2017; Revised version received: March 14, 2017; Accepted: March 16, 2017; Published: March 27, 2017.

DOI: 10.15376/biores.12.2.3530-3545